Double circular erosion patterns on dielectric target in magnetron sputtering

Yoshifumi Suzaki, Hayato Miyagawa, and Seiki Ejima
Department of Advanced Materials Science, Kagawa University, 2217-20 Hayashi-cho, Takamatsu, Kagawa 761-0396, Japan

(Received 25 April 2009; accepted 24 August 2009; published online 13 October 2009)

In rf magnetron sputtering, a circular erosion pattern forms on the surface of a circular metal conductor target with permanent magnets on its back. In this case, the theory behind the erosion pattern has been established. However, in the case of a dielectric target, a double circular erosion pattern is formed. So far, this pattern has been phenomenologically recognized by experimenters; however, it has not yet been investigated. In this study, we performed a magnetron sputtering experiment with a SiO_2 dielectric target, and confirmed the formation of a double circular erosion pattern. The dimensions of the double circular erosion pattern varied depending on the insulation resistance or the thickness of the SiO_2 target. Furthermore, we found that the dimensions of a double circular erosion pattern changed by making a gap between the SiO_2 target and guard ring. Based on the experimental results, we have proposed a qualitative model to explain the formation mechanism of double circular erosion patterns. © *2009 American Institute of Physics.* [doi:10.1063/1.3227236]

I. INTRODUCTION

The magnetron sputtering method is generally used for the fabrication of films. Film thickness distribution changes in relation to the distance between the target and the substrate; thus, fabrication of a uniform film continues to be a subject of investigation. Moreover, because of the permanent magnets on the backside of the target, the erosion of the target by sputtering is not uniform, and the depth of the erosion is different along the magnetic field.[1,2] This makes it difficult to use the target effectively. In order to improve the utilization rate of the target, many recent attempts have been made.[3,4]

In rf magnetron sputtering, a circular erosion pattern is formed on the surface of the circular metal conductor target with permanent magnets behind the target, as shown in Fig. 1. The theory behind the formation of this erosion pattern has been established.[5,6] However, in the case of a dielectric target, a double circular erosion pattern is formed. So far, this pattern has been phenomenologically recognized by experimenters; however, it has not yet been investigated. The dimensions of the erosion patterns may vary in relation to the thickness of the dielectric target, so that insulation resistance is different.

In this study, we perform a magnetron sputtering experiment with a SiO_2 dielectric target, and confirm the formation of a double circular erosion pattern. Based on the experimental results, we propose a qualitative model to explain the formation mechanism of double circular erosion patterns for designing the sputtering system with high utilization rate.

II. CONDITION OF THE TARGET

In our experiment, the thickness of the target was changed by combining SiO_2 and Cu targets 1 mm thick. A double circular erosion pattern was measured by changing the thickness of the target. The diameter of the target is 70 mm. A schematic diagram of the placement of the target is shown in Fig. 2. Using a target consisting of a combination of SiO_2 targets and Cu targets we measured how the double circular erosion pattern changes. Patterns of the combinations of the targets are shown in Table I. Here, *S* indicates the SiO_2 target, *C* indicates the Cu target, and *G* indicates the gap shown in Fig. 2, where there is a distance of 5 mm between the metal electrode and the guard ring. A combination of targets 1 mm thick was set for measuring differences in erosion. Moreover, the change in erosion when there is a gap between the guard ring and the surface of the target was measured. The purity, electrical conductivity, and dielectric constant of the SiO_2 target were 99.99%, less than 10^{-18} $(\Omega\ \mathrm{m})^{-1}$ and 3.8.

We used a noncontact three dimension measuring system (Ryokosha Corp., NH-3N) for the measurement of the target erosion pattern. A measurement of three directions along the diameter via the center of the target was performed. A profile and view of erosion on the metal conductor (Cu) target, which was performed for comparison, are shown in Figs.

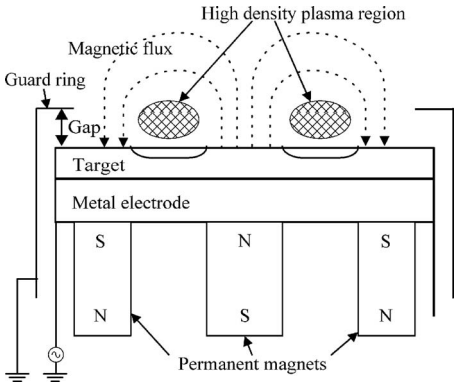

FIG. 1. Schematic design of the target. Because of the permanent magnets on the backside of the target, the erosion of the targets by sputtering is not uniform, and the depth of the erosion is different along the magnetic field.

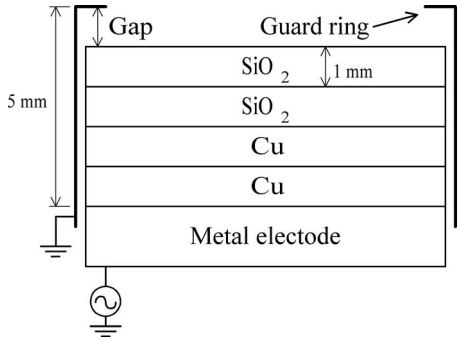

FIG. 2. Schematic diagram of the placement of the target. The diameter of the target is 70 mm. The thickness of the target was changed by combining SiO_2 targets and Cu targets 1 mm thick.

3(a) and 3(b), respectively. The condition of the sputtering was high frequency electricity (13.56 MHz, 200 W), and the accumulated electric discharge time was 150 h. In Fig. 3(a), a typical single circular erosion pattern on the metal conductive target was confirmed. Moreover, clear erosion is shown in Fig. 3(b). In a magnetron sputtering system, electrons are trapped by the magnetic field and high density plasma is created in the narrow circle-shaped region near the target surface. A single circular erosion pattern is formed under this region because the sputtering rate is higher than the value under the other region.

III. RESULTS OF MEASUREMENTS OF THE TARGET EROSION PATTERN

Conditions of sputtering in the dielectric target were the power of rf supply (200 W), reflection electricity at less than 1%, and the discharge time at 2 h. A typical photo of the double circular erosion pattern on the surface of the SiO_2 target provided by the experiment is shown in Fig. 4. This erosion pattern is clearly different from the one in Fig. 3(b). A profile measurement was performed for this pattern. Results of the measurement of the erosion pattern profile of the target are as follows. In this paper, we defined a double circular erosion pattern as having two local maximums in a circle-shaped erosion pattern.

The relationship between thickness of SiO_2 (S) and the erosion pattern, with a constant gap $G=0$, is shown in Fig. 5.

TABLE I. A combination of the targets: Cu and SiO_2. S indicates the SiO_2 target, C indicates the Cu target, and G indicates the gap shown in Fig. 2.

Sign	SiO_2 (mm)	Cu (mm)	Gap (mm)
S5	5	0	0
S4G1	4	0	1
S4C1	4	1	0
S3C1G1	3	1	1
S3C2	3	2	0
S3G2	3	0	2
S2C2G1	2	2	1
S2C3	2	3	0
S2G3	2	0	3
S2C1G2	2	1	2
S1G4	1	0	4
S1C1G3	1	1	3
S1C2G2	1	2	2
S1C3G1	1	3	1
S1C4	1	4	0

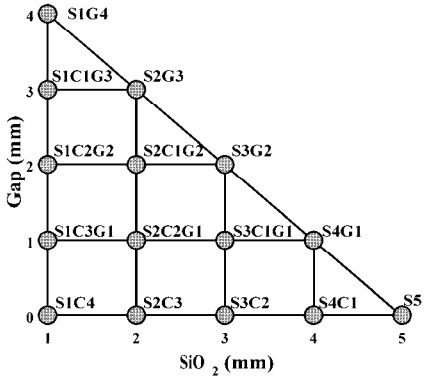

Figure 5(a) shows erosion depth profiles on the targets. In S1C4, deep erosion occurred in the circle-shaped area where plasma density was high. Erosion depth became shallower as S increased. In S2C3, erosion depth was about half as deep as in S1C4. Moreover, the shape of the erosion was distorted

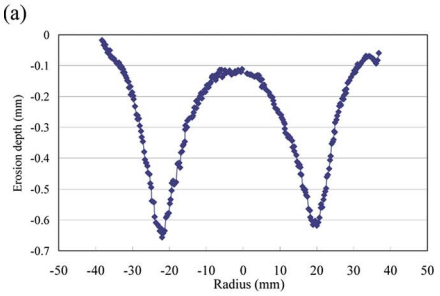

FIG. 3. (Color online) Erosion on the metal conductor (Cu) target. (a) and (b) show a profile and a photo of the erosion on the surface. The condition of the sputtering was high frequency electricity (200 W), and the accumulated electric discharge time was 150 h. A typical single circular erosion pattern was confirmed on the target.

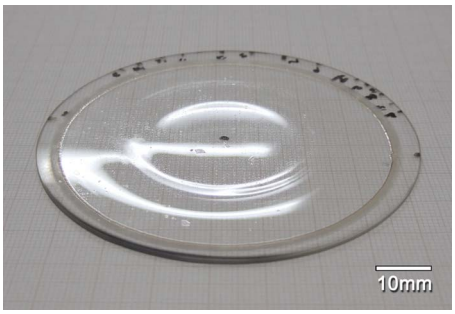

FIG. 4. (Color online) Typical photo of the double circular ring of erosion on the surface of the SiO_2 target. The erosion pattern is clearly different from the one in Fig. 3(b).

but had only one maximum. Its distorted depth profile will be discussed later. In S3C2, S4C1, and S5, erosion depth profiles had two local maximums in a circle-shaped erosion pattern. The formation of a double circular erosion pattern was confirmed at $S=3$, 4, and 5 mm; a single circular erosion pattern was present at $S=1$ and 2 mm. Figure 5(b) shows relations between S and the radius of the double circular erosion pattern. S increased, and the radius of the inner and outer circular erosion patterns decreased and increased, respectively. The difference of the radius of the two circular erosion patterns increased.

The relationship between thickness of SiO_2 (S) and the erosion pattern, with a constant gap $G=1$ mm, is shown in Fig. 6. Figures 6(a) and 6(b) show erosion depth profiles on the targets and radius of the double circular erosion patterns, respectively. In Fig. 6(a), erosion depth at $S=1$ was more than three times as deep as at the other three profiles. At $S=2-4$ mm, the erosion depth decreased linearly with an increase in S. In Fig. 6(b), the formation of a double circular

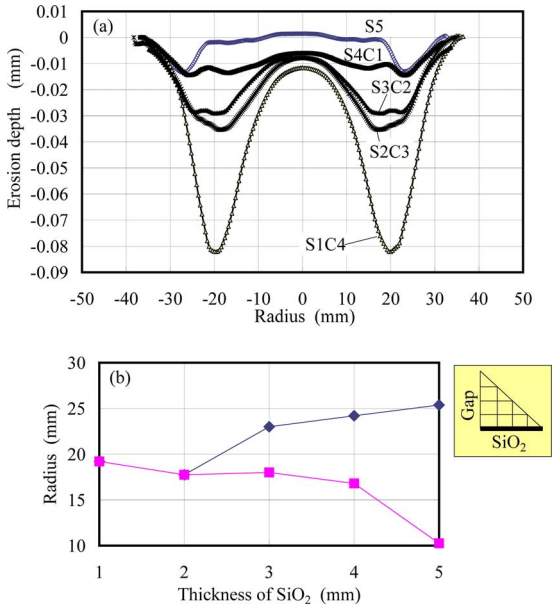

FIG. 5. (Color online) Relationship between thickness of SiO_2 (S) and the erosion pattern, with a constant gap $G=0$. (a) shows erosion depth profiles on the targets. Deep erosion occurred in the circle-shaped area where plasma density was high. (b) shows the relations between S and the radius of the double circular erosion pattern. The triangular diagrams in these figures are the same as in Table I.

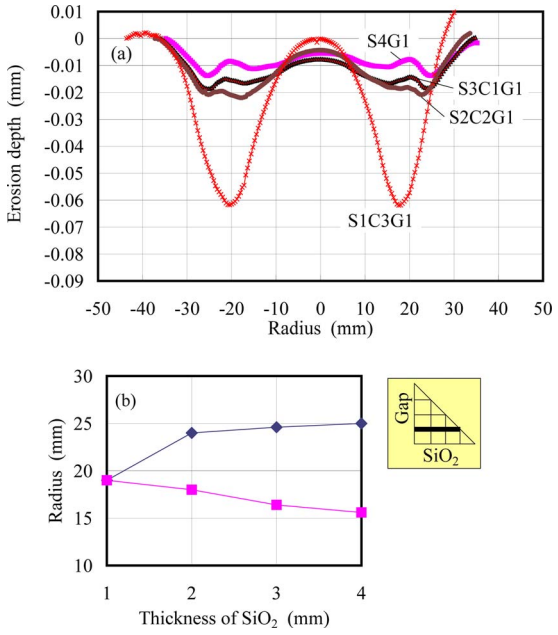

FIG. 6. (Color online) The relationship between thickness of SiO_2 (S) and the erosion pattern, with a constant gap $G=1$ mm. (a) and (b) show erosion depth profiles on the targets and radius of the double circular erosion patterns, respectively.

erosion pattern was confirmed, except in the case of $S=1$ mm. In the case of $G=1$ mm, a double circular erosion pattern was formed at $S=2$, 3, and 4 mm, whereas a double circular erosion pattern was formed at $S=3$ and 4 mm, with $G=0$. This difference may depend on the influence of the size of G.

For S fixed at 1 mm, and G changed from 0 to 4 mm, the erosion profile results are shown in Fig. 7. Figures 7(a) and 7(b) show erosion depth profiles on the targets and radius of

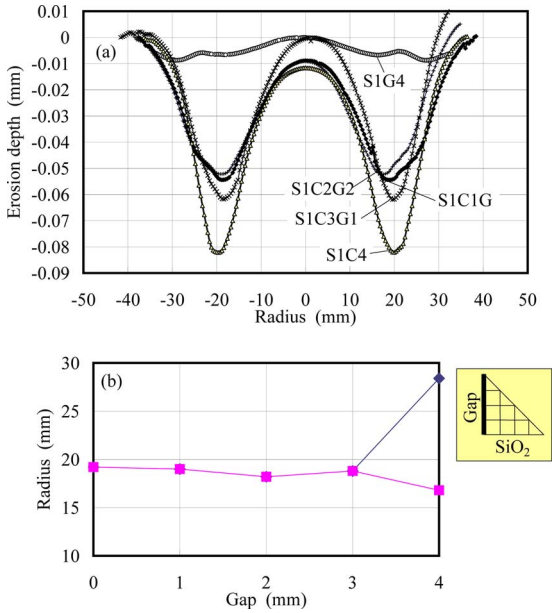

FIG. 7. (Color online) The relationship between the gap (G) and the erosion pattern, with a constant thickness of SiO_2 $S=1$ mm. (a) and (b) show erosion depth profiles on the targets and radius of the circular erosion patterns, respectively. A double circular erosion pattern did not appear when $G=0-3$ mm.

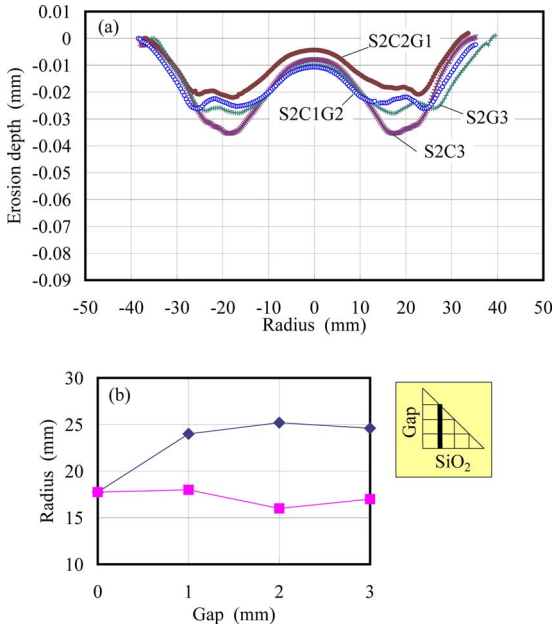

FIG. 8. (Color online) The relationship between the gap (G) and erosion pattern, with a constant thickness of SiO_2 $S=2$ mm. (a) and (b) show erosion depth profiles on the targets and radius of the double circular erosion patterns, respectively. In the case of $G=1-3$ mm, the formation of a double circular erosion pattern was confirmed, although not in the case of $G=0$. The radius of the inner circular erosion pattern was constant; therefore, the radius of the outer pattern increased as G increased.

the double circular erosion patterns, respectively. In Fig. 7(a), erosion depth is deepest at $G=0$. Erosion depth is approximately constant in the case of $G=1-3$ mm. The erosion depth is extremely shallow in the case of $G=4$ mm. The erosion pattern changes whether there is a gap or not. The size of G may not have an influence on the erosion pattern. Because the size of S was much smaller than G, at $G=4$ mm, the reason why the erosion depth became shallow thought to be because the Ar^+ ions may have gone greatly astray into the guard ring side. In Fig. 7(b), the formation of a double circular erosion pattern was confirmed at $G=4$ mm. Therefore, at $G=0$, the target was eroded like a conductive target and a double circular erosion pattern did not appear. On the other hand, at $G=1-3$ mm, the target was eroded irregularly; therefore, a double circular erosion pattern did not appear. This pattern will be discussed later.

The relationship between the gap (G) and the erosion pattern, with a constant thickness of SiO_2 $S=2$ mm is shown in Fig. 8. Figures 8(a) and 8(b) show erosion depth profiles on the targets and radius of the double circular erosion patterns, respectively. In Fig. 8(a), when $G=0$, the target was eroded greatly. In the case of $G=1-3$ mm, the erosion depth was smaller than at $G=0$, and grew deeper linearly as the size of G increased. In Fig. 8(b), in the case of $G=1-3$ mm, the formation of a double circular erosion pattern was confirmed, except in the case of $G=0$. The radius of the inner circular erosion pattern was constant; therefore, the radius of the outer pattern increased as G increased.

IV. DISCUSSION

Using a metal conductive target, a single circular erosion pattern was formed on the surface of the target after sputtering. It was caused because there was a circular high-density sputtering electric discharge near the surface of the target due to the permanent magnets on the back of the target. This phenomenon has already been observed and described theoretically. In this paper, we confirm that the Cu target was eroded in the shape of a circle [Fig. 3(b)].

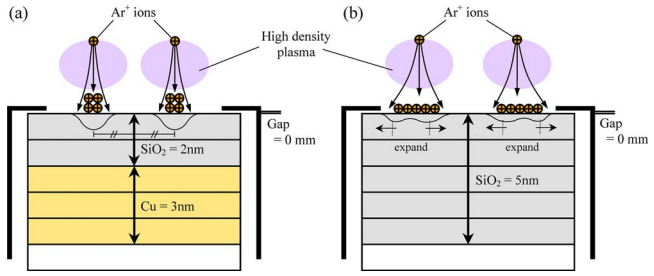

FIG. 9. (Color online) Two models of sputtering of the target at different thicknesses of SiO_2; (a) $S=2$ mm and (b) 5 mm with a constant value of $G=0$. When $S=2$ mm in (a), a deep single circular erosion pattern appeared. However, when $S=5$ mm in (b), a shallow double circular erosion pattern appeared instead because the size of the charged domain was larger.

However, the formation of a double circular erosion pattern was confirmed on the surface of the dielectric target (Fig. 4). Because the Ar^+ ions that reached the target surface are not neutralized, the target surface is charged positively, and, as a result, Ar^+ ions avoided a charged domain through Coulomb repulsion. Moreover, a double circular erosion pattern was formed. The erosion patterns were different when the states of the insulation resistance varied with the thickness of the dielectric target. We changed the thickness of SiO_2 from 1 to 5 mm and measured the erosion on the surface of the target after sputtering. In Fig. 5(a), insulation resistance increased with the thickness of SiO_2, and the erosion depth on the target decreased. A double circular erosion pattern was not formed on 1 mm thick SiO_2, but was formed on over 2 mm thick SiO_2. In addition, the distance between the two circles of erosion increased with the thickness of SiO_2 [Fig. 5(b)]. The thickness of the dielectric target increased, thus insulation resistance of the surface of the target increased; as a result, the target surface became more positively charged. Based on these results, we developed two models of sputtering of the target at different thicknesses of SiO_2; 2 and 5 mm, as shown in Fig. 9. With thin SiO_2, the charged domain was narrow because there was little quantity of Ar^+ charged on the surface, and, as a result, a distinct double circular erosion pattern did not appear. However, the erosion depth was deep because of the small quantity of the electrical charge.

Moreover, in the experiment, when there was a gap between the target and the guard ring as shown in Fig. 2, different double circular erosion patterns with different depths were formed. Because the guard ring was connected to the cathode, it was thought that Ar^+ ions were led to the guard ring side when the gap was large.

When the gap was fixed ($G=1$ mm) and the thickness of SiO_2 was changed, the results are shown in Figs. 6(a) and 6(b). Comparing Fig. 6(a) with Fig. 5(a), when $G=0$ and 1 mm, a double circular erosion pattern was formed when the thickness of SiO_2 was more than 3 and 2 mm, respectively.

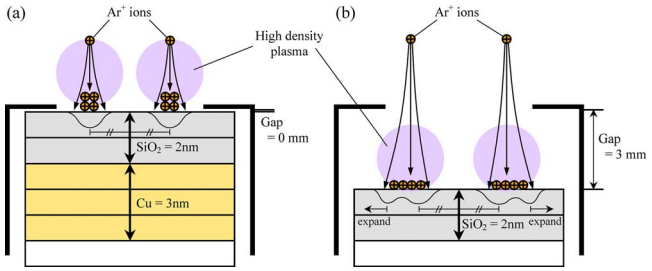

FIG. 10. (Color online) Schematic diagrams of the single and double circular rings of erosion at different gaps, (a) $G=0$ and (b) 3 mm with a constant value of $S=2$ mm. When $G=0$ in (a), the double circular erosion pattern was not formed. However, when $G=3$ mm in (b), because the flow of the Ar^+ ion spreads toward the guard ring side, and the size of the charged domain became larger, a double circular erosion pattern was formed instead.

These results show that Ar^+ ions flow through the guard ring side when a gap is made. Consequently, when the thickness of SiO_2 was constant and the gap was 0–4 mm, a double circular erosion pattern did not appear clearly. When SiO_2 was 1 mm thick, and the gap was increased, the erosion depth became shallow; in addition, a double circular erosion pattern tended to form, as shown in Figs. 7(a) and 7(b). This result shows that Ar^+ ions were not accumulated in the target neighborhood very much at 1 mm because insulation resistance was low. When the gap was increased, Ar^+ ions led to the guard ring side increased; as a result, a double circular erosion pattern was formed. Furthermore, at 2 mm of SiO_2, when there was not a gap ($G=0$), the erosion was deep, but a double circular erosion pattern did not appear, as shown in Figs. 8(a) and 8(b). However, when there was a gap, the erosion depth was shallower than the depth without a gap. In addition, the radius of the inner circle did not depend on the gap size. However, the radius of the outer circle increased as the gap size increased. Figure 10 shows schematic diagrams of the single and double circular rings of erosion at different gaps, (a) $G=0$ and (b) 3 mm. When there is not a gap, as shown in Fig. 10(a), the spread of the Ar^+ ions was narrow, and a charged domain on the surface of the target was small. Thus, a double circular erosion pattern was not formed, and the erosion depth was deep. When there was a gap, as shown in Fig. 10(b), the flow of the Ar^+ ion spreads toward the guard ring side, and the charged domain was wide. A double circular erosion pattern was thus formed, and the erosion depth was shallow.

S1C4 showed a single circular erosion pattern in Fig. 5 because insulation resistance of 1 mm thick SiO_2 is low. In S2C3 (in Fig. 5) and S1C3G1 (in Fig. 7), the erosion depths were shallower than in S1C4. Moreover, the erosion profiles were distorted but had only one maximum value. These distortions seem to be caused by surface charge. We will discuss these two combination targets. The simple fitting function for the erosion shape for metal targets was introduced through the concept of a virtual line source in a collisionless plasma by Kusumoto and Iwata,[6] They assumed a two-dimensional Maxwellian source of temperature T, located at the distance h from the target surface in a uniform electric field E. Then the incident flux distribution $n(x)$ could be obtained as follows:

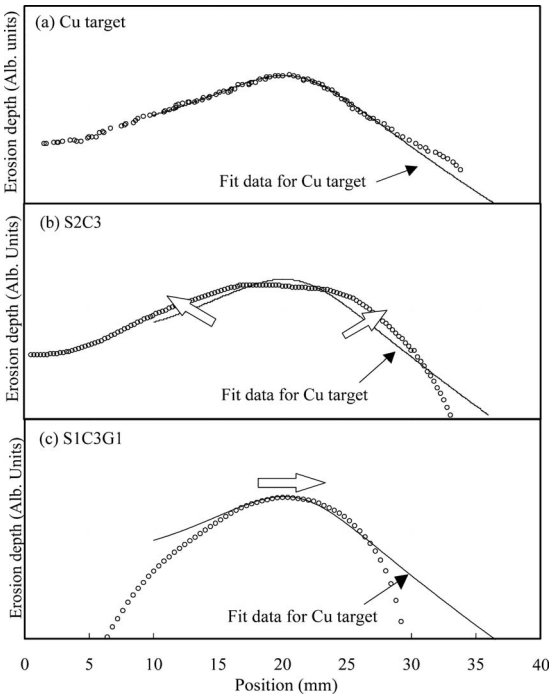

FIG. 11. Fittings of experimental erosion depth data for (a) the Cu target, (b) S2C3 and S1C3G1 using Eq. (1) by Kusumoto and Iwata (Ref. 6). For the Cu target in (a), the calculated data indicated by the solid line corresponded closely to experimental data indicated by open circles across the eroded region. For S2C3 in (b), erosion depth at the center is shallower than the solid line [the same line as in (a)]. Moreover in (b), the erosion center widened at both the inner and outer sides. However in (c), erosion depth at the outer side is deeper than the solid line. These two tendencies are consistent with the prediction made regarding by the models in Figs. 9 and 10.

$$ndx \approx \sqrt{\frac{\beta}{8\pi}}\frac{e^{\beta(1-r)}}{r}\left(\sqrt{r}+\frac{1}{\sqrt{r}}\right)d\xi, \tag{1}$$

where r, ξ, and β are defined by

$$r=\sqrt{1+\xi^2}, \quad \xi=\frac{(x-m)}{h} \quad \text{and} \quad \beta=\frac{qEh}{2kT}, \tag{2}$$

respectively. m is the position of the erosion center. k and q denote the Boltzmann constant and elementary electric charge. Figure 11(a) shows the fit of calculated erosion depth data using Eq. (1) in semilogarithmic plots for a Cu target. The calculated data indicated by the solid line correspond closely to the experimental data indicated by open circles across the eroded region. Figures 11(b) and 11(c) show experimental data of S2C3 and S3C3G1, respectively. The solid lines in Fig. 11(b) and 11(c) are the calculated data for the Cu target, which is the same as the data in Fig. 11(a). For S2C3 in Fig. 11(b), erosion depth at the center is shallower than the solid line, and the erosion center widened at both the inner and outer sides. This result was caused by an increase in electric charge at the center of erosion. As the electric charge increases, the profile is expected to change from a single circular pattern to a distorted pattern, and finally to a double circular pattern. However, for S1C3G1 in Fig. 11(c), erosion depth at the outer side is deeper than the solid line. This result was caused by the gap between the guard ring and the surface of the target. These two tendencies are consistent

with the prediction made regarding by the models in Figs. 9 and 10.

V. CONCLUSION

In this study, we performed a magnetron sputtering experiment on a SiO_2 dielectric target and were able to confirm the formation of a double circular erosion pattern, which agreed with qualitative theory. Moreover, insulation resistance varied with the thickness of the SiO_2 target; thus the dimensions of a double circular erosion pattern also varied. Furthermore, we confirmed in the experiments that the depth of a double circular erosion pattern changed by making a gap between the SiO_2 target and guard ring. Results are summarized as follows.

(1) The erosion depth is shallow when SiO_2 is thick or the gap is large. On the contrary, the erosion depth is deep when SiO_2 is thin or the gap is small.
(2) When SiO_2 is thick because the insulation resistance is high the erosion depth is shallow. Moreover, when the gap is large because Ar^+ ions are led to the guard ring side, and the charged domain of the Ar^+ ions becomes large, the erosion depth decreases.
(3) When the SiO_2 is thin or the gap is small, a single circular erosion pattern is formed. Under these conditions, a double circular erosion pattern is formed.

These results suggest that thickness and dimensions of the gap in an SiO_2 target should be balanced to achieve a deep erosion depth and a double circular erosion pattern. Thus, the most suitable condition in our equipment was SiO_2 at 2 mm, and the gap at 3 mm. The sputtering system with the maximum utilization rate of the dielectric target can be designed by using the obtained fundamental results.

In this study, on a dielectric target, the formation of a double circular erosion pattern was confirmed; this agreed with qualitative theory. In addition, we will examine double circular erosion patterns that are caused by making a gap between a target and guard ring, and will formulate a theory about these results in the future.

ACKNOWLEDGMENTS

We thank Mr. Ian Willey for his careful proofreading of our manuscript.

[1] T. Iseki, H. Maeda, and T. Itoh, Vacuum **82**, 1162 (2008).
[2] K. Kohler, J. W. Coburn, D. E. Horne, and E. Kay, J. Appl. Phys. **57**, 59 (1985).
[3] T. Iseki, H. Maeda, and T. Itoh, Vacuum **83**, 470 (2008).
[4] S. Schiller, U. Heisig, and K. Goedicke, J. Vac. Sci. Technol. **14**, 815 (1977).
[5] K. Okazawa, E. Shidoji, and T. Makabe, J. Appl. Phys. **86**, 2984 (1999).
[6] Y. Kusumoto and K. Iwata, Vacuum **74**, 359 (2004).